Contrib. Astron. Obs. Skalnaté Pleso **41**, 106 – 112, (2011)

Synoptic charts of solar magnetic fields

M. Minarovjech, V. Rušin and M. Saniga

Astronomical Institute of the Slovak Academy of Sciences
059 60 Tatranská Lomnica, The Slovak Republic

Received: March 7, 2011; Accepted: April 15, 2011

Abstract. Time-latitude and time-longitude distributions of solar surface magnetic fields are analyzed employing classical and modified synoptic charts. The equatorial branch in solar cycle 23 in the southern hemisphere lasted two years longer than its northern counterpart. The most remarkable finding is that in the present solar cycle a pole-ward migrating magnetic field branch is absent on the southern hemisphere, while on the northern one is well developed. This feature was not observed in previous solar cycles for the same period after cycles' onsets.

Key words: Sun: solar cycle – Sun: synoptic charts of magnetic fields

1. Introduction

Solar surface magnetic fields play a crucial role in solar activity and solar terrestrial relations. Since their discovery by Hale in 1908, their measurements and observing techniques have made a big progress. Currently, they are measured routinely on a daily basis, which allows us to prepare their synoptic charts and thus study their distribution across the solar globe as well as their temporal evolution on par with other pronounced phenomena of solar activity, like sunspots, prominences, *etc.*

In the present paper we will study synoptic charts of longitudinally-measured magnetic fields in the solar photosphere for the period from 1975 to 2011 (which corresponds to Carrington rotations (CR) 1625–2107). A time-latitude and time-longitude evolutions of surface magnetic fields are shown and discussed.

2. Observational data

The data used for this study comprise three basic sets of synoptic charts. The first one is the data set of all available NSO/Kitt Peak synoptic magnetogram maps (`ftp://nsokp.nso.edu/kpvt/synoptic/mag/`) in a form of 180×360 arrays from CR 1625 (1975.13) to CR 2006 (2003.66). The missing data for the period from CR 1640 to CR 1644, as well as for CR 1854, were supplied by interpolation. The second set comprises net (signed) flux frames of magnetic synoptic FITS files obtained by the Vector Spectromagnetograph (VSM), which is part of NSOs Synoptic Optical Long-term Investigations of the Sun (SOLIS) instrumental package (`ftp://solarch.tuc.noao.edu/synoptic/level3/vsm/`

`merged/carr-rot/`); the corresponding period is from CR 2007 to CR 2105. The final set is represented by SOHO/MDI magnetic field synoptic charts (`http://soi.stanford.edu/magnetic/index6.html`) for the period from CR 1909 (1996.34) to CR 2051 (2007.02). All SOHO/MDI synoptic magnetogram maps were likewise interpolated into 180×360 data arrays; these data are, after a rescaling, also used to supply the missing VSM data.

3. Results

Due to a lack of space, we shall only show a couple of charts that illustrate sufficiently well time-latitude distributions of longitudinally-averaged solar surface magnetic fields: the first one (Fig. 1) is a "classical" presentation, whilst the other (Fig. 2) is a "modified" one. The detailed treatise on how these maps were computed and the reasons that led to the "modified" view can be found in Minarovjech (2008) and Minarovjech *et al.* (2008). From both the figures one immediately discerns a Butterfly diagram similar to the standard Butterfly diagram of the latitude of sunspot occurrence versus time. Although this diagram is most pronounced in low and middle latitudes, its traces can be found, unlike sunspots, even in the regions close to the poles (in particular in Fig. 2). A careful inspection of the figures reveals that:

– The boundaries between the regions of different polarity are very well pronounced.

– Their evolution can easily be discerned; one clearly sees both pole-ward migrating and equatorial branches.

– In the former case, in addition to primary branches, we also observe less developed, second branches, which move a bit faster (see Fig. 2; branches marked by black arrows). As a side note, it is worth mentioning that the existence of two kinds of polar branches is typical also for prominences; *e.g.*, Waldmeier (1973), Dermendjiev *et al.* (1994), and McIntosh (2003).

– In cycle 23, the northern equatorial branch reached the equator a couple of years earlier than its southern counterpart.

– The current cycle (24) features a well-developed, primary polar branch on the northern hemisphere (see Fig. 2; the branch marked by a white arrow), yet it lacks its southern counterpart. No previous cycle exhibited such an "anomaly."

If the values of magnetic field strength from synoptic charts are averaged along latitudes, one gets a picture like that depicted in Fig. 3; the method employed to get this figure is identical with that described in Minarovjech (2008), the only difference being that now averaging is done along latitudes. Such a chart carries very important information about the differential rotation of the

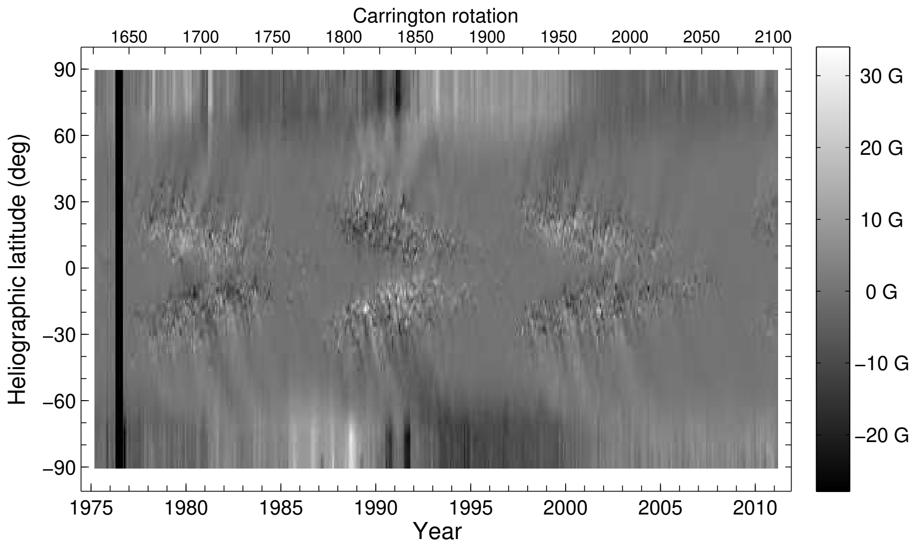

Figure 1. A time-latitude distribution of the longitudinally-averaged photospheric magnetic field strength for the period from 1975 to 2010 — a classical view. The strength of magnetic fields is indicated by a grayscale bar.

Table 1. The mean values of the Sun's rotational velocity (days) for individual cycles under study, shown separately for ascending and descending periods.

Cycle	21	22	23	24
Ascending period	27.6 ± 0.1	27.7 ± 0.1	27.7 ± 0.1	27.96 ± 0.1
Descending period	26.8 ± 0.1	26.8 ± 0.1	26.7 ± 0.1	—

Sun and proper motion of long-living active magnetic regions; the differential rotation is inferred from the inclinations of white strips (which are better visible in Fig. 4) with respect to the vertical/horizontal line. Fig. 3 can also serve as a nice illustration of the well-known fact that the Sun's rotational velocity is different for ascending and descending periods of solar cycles, as listed explicitly in Tab. 1.

The averaging of the data shown in Fig. 3 (and so in Tab. 1) was done in the full range of latitudes. If one considers an averaging with a finer step and within a smaller range, ±60 degrees, we get a little different pattern — Fig. 4. Here, for a better illustration, we divided the interval into 8 sectors/belts of 15 degrees each. The corresponding mean values of the rotational velocity for each sector are given in Tab. 2.

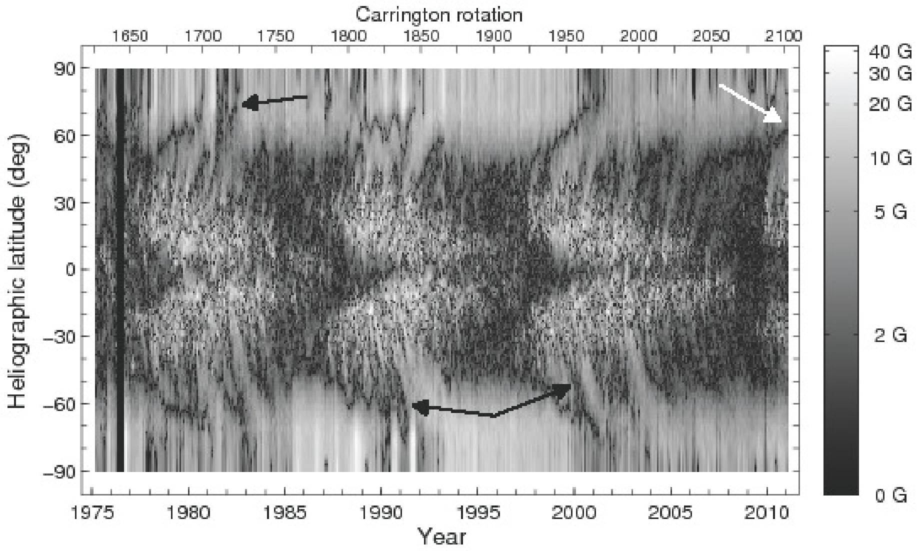

Figure 2. A time-latitude distribution of the absolute values of the longitudinally-averaged photospheric magnetic field strength for the period from 1975 to 2010 — a modified view.

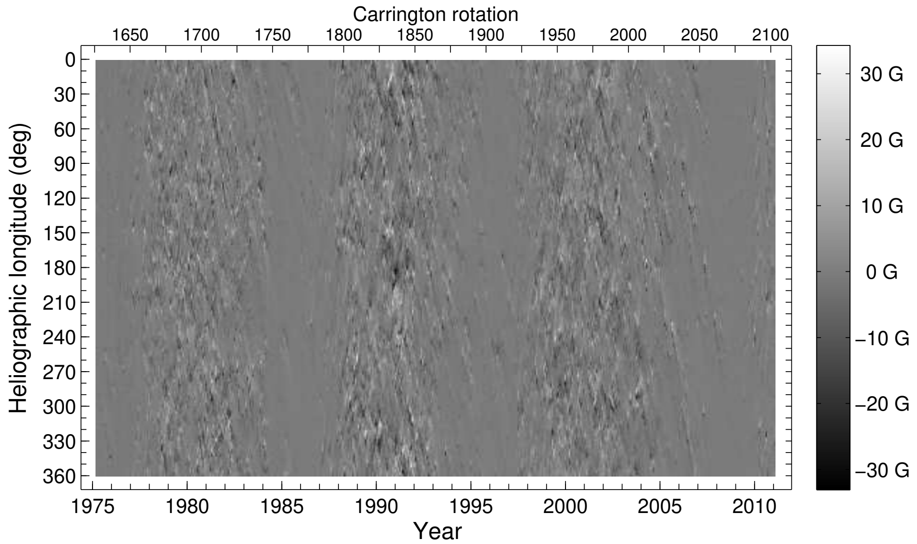

Figure 3. A time-longitude distribution of the latitudinally-averaged photospheric magnetic field strength for the period from 1975 to 2010. The strength of magnetic fields is indicated by a grayscale bar.

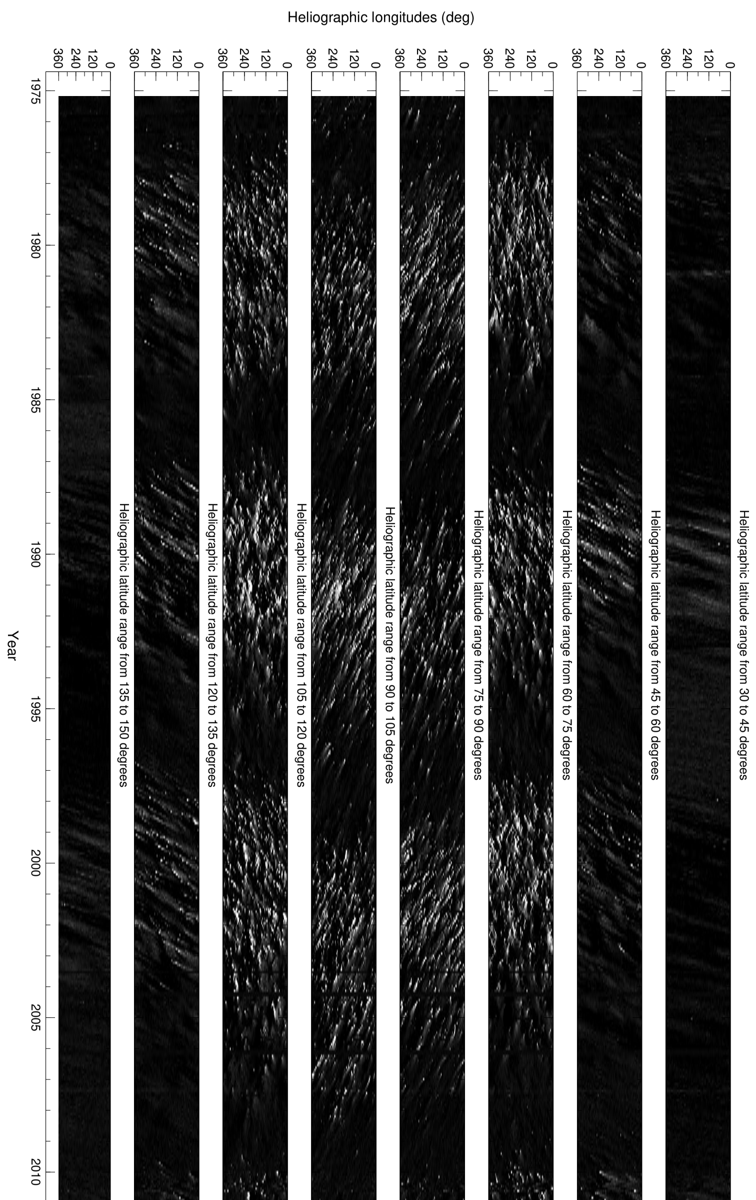

Figure 4. The same as in the preceding figure, but employing a different kind of magnetic field strength averaging. Bright and dark strips represent magnetically active regions. The "tilting" of individual strips is proportional to the average rotational velocity in a particular belt. (Note: Latitude is here expressed in terms of positional angles.)

Table 2. Rotational rates for individual heliographic belts and cycles.

PA/Cycle	21	22	23	24
$30-45$	$31.6+2.2(-1.1)$	$30.7+1.7(-0.9)$	$30.6+1.3(-0.8)$	$30.8+1.4(-0.8)$
$45-60$	28.5 ± 0.1	$28.9+0.9(-0.5)$	$28.8+0.1(-0.5)$	$29.5+0.7(-0.5)$
$60-75$	27.3 ± 0.4	27.4 ± 0.4	27.3 ± 0.4	27.3 ± 0.4
$75-90$	26.8 ± 0.1	26.8 ± 0.1	26.8 ± 0.1	—
$90-105$	26.8 ± 0.1	26.8 ± 0.1	26.8 ± 0.1	—
$105-120$	$27.7+0.7(-0.5)$	27.3 ± 0.2	$27.7+0.5(-0.7)$	27.2 ± 0.4
$120-135$	$28.9+0.6(-0.9)$	$28.5+0.4(-0.3)$	$29.1+0.8(-0.5)$	$28.7+1.6(-0.7)$
$135-150$	$30.9+1.3(-0.8)$	$31.8+1.3(-1.4)$	$30.5+1.3(-0.7)$	$30.4+1.3(-0.7)$

4. Discussion and conclusion

We have carried out a brief analysis of the time-latitude and time-longitude distributions of the longitudinally-averaged component of the solar surface magnetic field strength within the period from 1975 to 2010, which covers three full solar cycles (21 to 23) and the onset of cycle 24. Our study was based on the so-called modified synoptic charts of magnetic fields as described in Minarovjech (2008). One clearly sees both pole-ward migrating and equatorial branches; in the former case, in addition to primary branches, we also observe less-developed, secondary branches, which move a bit faster. In cycle 23, the northern equatorial branch reached the equator a couple of years earlier than its southern counterpart. The current cycle (24) features a well-developed, primary polar branch on the northern hemisphere, yet it lacks its southern counterpart. No previous cycle exhibited such an "anomaly." We have also confirmed the well-known fact that the Sun's rotational velocity is different for ascending and descending periods of solar cycles, as listed explicitly in Tabs. 1 and 2 for two different kinds of magnetic field strength averaging. Although their origin is still far from being properly understood (Hathaway, 2010), it is a generally held view that magnetic fields are the main agent behind solar activity. This is nicely illustrated by the above-mentioned findings when combined with those based on observations of prominences and green line corona (Minarovjech *et al.*, 2011). All these phenomena seem to be intimately linked to the large-scale meridional circulation on the surface of the Sun, when plasma moves from the equator to the poles at a velocity of about 10-15 $\mathrm{m\,s^{-1}}$, this velocity being different for ascending and descending periods of solar cycles (Hathaway and Rightmire, 2010). Our findings are hoped to contribute to getting further insights into the nature of solar activity and its link with space weather.

Acknowledgements. This work was fully supported by the Slovak Academy of Sciences VEGA project 2/0098/10.

References

Dermendjiev, V.N., Stavrev, K.Y., Rušin, V., Rybanský, M.: 1994, *Astron. Astrophys.* **281**, 241

Hathaway, D.H.: 2010, *Living Reviews in Solar Physics* **7**, 1

Hathaway, D.H., Rightmire, L.: 2010, *Science* **327**, 1350

McIntosh, P.S.: 2003, in *Proc. Solar Variability as an Input to the Earth's Environment*, ed.: A. Wilson, ESA SP, **535**, 807

Minarovjech, M.: 2008, *Contrib. Astron. Obs. Skalnaté Pleso* **38**, 5

Minarovjech, M., Rušin, V., Saniga, M.: 2008, *Sol. Phys.* **248**, 167

Minarovjech, M., Rušin, V., Saniga, M.: 2011, *Contrib. Astron. Obs. Skalnaté Pleso* **41**, 175

Waldmeier, M.: 1973, *Sol. Phys.* **28**, 389